Pharmaceutical Research, Vol. 25, No. 10, October 2008 (© 2008)
DOI: 10.1007/s11095-008-9628-x

Research Paper

Elastase-Sensitive Elastomeric Scaffolds with Variable Anisotropy for Soft Tissue Engineering

Jianjun Guan,[1,4] Kazuro L. Fujimoto,[1] and William R. Wagner[1,2,3,5]

Received March 10, 2008; accepted May 6, 2008; published online May 29, 2008

Purpose. To develop elastase-sensitive polyurethane scaffolds that would be applicable to the engineering of mechanically active soft tissues.
Methods. A polyurethane containing an elastase-sensitive peptide sequence was processed into scaffolds by thermally induced phase separation. Processing conditions were manipulated to alter scaffold properties and anisotropy. The scaffold's mechanical properties, degradation, and cytocompatibility using muscle-derived stem cells were characterized. Scaffold *in vivo* degradation was evaluated by subcutaneous implantation.
Results. When heat transfer was multidirectional, scaffolds had randomly oriented pores. Imposition of a heat transfer gradient resulted in oriented pores. Both scaffolds were flexible and relatively strong with mechanical properties dependent upon fabrication conditions such as solvent type, polymer concentration and quenching temperature. Oriented scaffolds exhibited anisotropic mechanical properties with greater tensile strength in the orientation direction. These scaffolds also supported muscle-derived stem cell growth more effectively than random scaffolds. The scaffolds expressed over 40% weight loss after 56 days in elastase containing buffer. Elastase-sensitive scaffolds were complete degraded after 8 weeks subcutaneous implantation in rats, markedly faster than similar polyurethanes that did not contain the peptide sequence.
Conclusion. The elastase-sensitive polyurethane scaffolds showed promise for application in soft tissue engineering where controlling scaffold mechanical properties and pore architecture are desirable.

KEY WORDS: anisotropy; elastase; polyurethanes; scaffolds; thermally induced phase separation.

INTRODUCTION

In the engineering of tissues, scaffolds serve as temporary mechanical supports to accommodate the growth and migration of seeded or infiltrating cells as the healing process proceeds. With the role of mechanical forces in tissue development and remodeling increasingly appreciated, the ability of scaffolds to provide an appropriate mechanical milieu for optimal tissue generation is an important consideration for scaffold design (1–4). Over time the scaffold should also degrade at a rate that allows growing tissue to gradually assume the mechanical load initially provided by the scaffold. When engineering mechanically active soft tissues such as cardiac muscle and blood vessels, elastic scaffolds are desirable since they might provide appropriate stress transfer during periods of loading and unloading.

The development of degradable and elastomeric polymers with properties appropriate for mechanically active tissue engineering has generated considerable interest (5–14). The majority of these polymers employ ester bonds for hydrolytic lability and can be thermoplastic or crosslinked elastomers. An advantage of thermoplastic over crosslinked polymers is the ability to process these materials by conventional approaches for 3D scaffold formation. Among thermoplastic elastomers, polyurethanes represent a major group. Hydrolytically labile polyurethanes with different soft and hard segments that possess various mechanical and biodegradation properties have been developed (5–10). Soft segments are often comprised of degradable polyesters or polycarbonates to introduce biodegradability. For the natural extracellular matrix, simple ester hydrolysis is not employed for remodeling, but rather numerous orchestrated enzymatic degradation pathways are triggered. To begin to mimic this process, enzymatically degradable polyurethanes have been developed by introducing enzyme sensitive peptides as chain extenders (5,9). In previously reported work, we developed families of polyurethanes using polycaprolactone and its copolymers as soft segments, 1,4-diisocyanatobutane as a hard segment and putrescine as chain extender (5–8). We further developed a family of elastase sensitive polyurethanes

[1] McGowan Institute for Regenerative Medicine, 100 Technology Drive, Pittsburgh, Pennsylvania 15219, USA.
[2] Department of Bioengineering, University of Pittsburgh, Pittsburgh, Pennsylvania 15261, USA.
[3] Department of Chemical Engineering, University of Pittsburgh, Pittsburgh, Pennsylvania 15261, USA.
[4] *Present address:* Department of Materials Science and Engineering, The Ohio State University, Columbus, Ohio 43210, USA.
[5] To whom correspondence should be addressed. (e-mail: wagnerwr@upmc.edu)

displaying both hydrolytic and elastase degradation mechanisms. Elastase lability was introduced in the polyurethane chain extension step by using the diamine peptide Ala–Ala–Lys (AAK) as a chain extender to react with the terminal isocyanates on the prepolymer. Elastase is able to cleave between the alanine residues (5).

The general objective of this work was to fabricate three dimensional porous scaffolds (~100 um pore size) suitable for soft tissue engineering from an elastase sensitive polyurethane. In considering how to process this thermoplastic elastomer into a scaffold, many methods could be utilized including electrospinning (15–17), solvent casting/salt leaching (9,18), phase inversion (19), laser excimer ablation (20) and thermally induced phase separation (21–26). All of these techniques except laser excimer ablation can be used to fabricate scaffolds with a random pore morphology. Randomly oriented porous scaffolds are suited to engineer tissues with uniform structural and mechanical properties. For engineering soft tissues that possess anisotropic structural and mechanical properties, scaffolds with oriented pores might be useful to guide tissue growth and mechanical transduction along preferred directions. Among the above mentioned methods, electrospinning, laser excimer ablation and thermally induced phase separation have been utilized to fabricate scaffolds with oriented pores. Electrospinning onto a rotating mandrel provides a method for generating fibrous scaffolds with control over the degree of fiber alignment and the resulting mechanical anisotropy (14–16). A disadvantage with this technique is that it is difficult to generate appropriate pore sizes for cellular ingrowth. Laser excimer ablation methods can generate straight pores in scaffolds, but achieving effective connectivity is a challenge (19). Thermally induced phase separation has previously been employed to fabricate gradient scaffolds (6,24,25). The pore size and morphology can be controlled by polymer concentration, quenching temperature, thermal gradient, and solvent type (24,25). Our previous experience employing thermally induced phase separation with similar thermoplastic elastomers (6) led us to evaluate the potential of this technique to be employed with an elastase sensitive polyurethane and to explore the potential for generating oriented pore scaffold morphologies. The effects of fabrication conditions such as heat transfer direction, solvent type, polymer concentration and quenching temperature on scaffold pore morphology and porosity were investigated. Scaffold mechanical properties and *in vitro* degradation were characterized. Scaffold cytocompatibility and support of cell growth were investigated for scaffolds with differing pore morphologies with muscle derived stem cells. Finally, we evaluated the *in vivo* degradation characteristics of an elastase sensitive polyurethane scaffold *versus* a similar polyurethane scaffold without elastase sensitivity in a subcutaneous rat implant model.

MATERIALS AND METHODS

Materials and Reagents

Polycaprolactone diol (PCL, MW 2000, Aldrich) was dried under vacuum overnight prior to synthesis. 1,4-Diisocyanatobutane (BDI, Fluka) and putrescine (Aldrich) were vacuum distilled before use. Stannous octoate (Sigma), H–Ala–Ala–Lys–OH (AAK, which contains two primary amines, Celtek Peptides, Inc.), anhydrous dimethyl sulfoxide (DMSO, Aldrich) and dimethylformamide (DMF, Aldrich) were used as received.

Synthesis of Elastase Sensitive Polyurethane

Polyurethaneurea (PU) containing the AAK sequence was synthesized by a two-step solution polymerization as previously described (5). In brief, 1.11 g (7.90 mmol) of BDI was added to a 250 ml three-necked round bottom flask equipped with Ar inlet and outlet. PCL (7.88 g, 3.95 mmol) was dissolved in 60 ml DMSO and then added into the flask under stirring. Two drops (approximately 22 mg) of stannous octoate [$Sn(OCt)_2$] were added and served as catalyst. The mixture was heated to 80°C and allowed to react for 3.5 h. A solution of AAK (11.39 g, 3.95 mmol) in DMSO was heated to 80°C and subsequently added to the prepolymer solution. The reaction was continued for 18 h at 80°C. The polymer solution was precipitated in an aqueous saturated potassium chloride solution. The resulting PU was dried under vacuum at 50°C for 24 h. The polymer was purified by precipitation of a PU in DMF solution in distilled water followed by vacuum drying.

Scaffold Fabrication

PU scaffolds with random and oriented pore morphologies were prepared using thermally induced phase separation as previously described for randomly oriented pore scaffolds (6). PU was dissolved in DMSO or dioxane at 80°C to form solutions with defined concentrations. PU solution was injected into a 10-mm diameter glass cylinder mold equipped with two rubber stoppers. The mold was thermally quenched at −20°C or −80°C for 3 h and then placed in 70% alcohol at 4°C for 7 days to extract the DMSO or dioxane. The scaffold was then immersed in water to extract ethanol followed by lyophilization.

To fabricate scaffolds with an oriented pore structure, a thermal gradient was applied during the thermally induced phase separation process, using a 25-ml beaker with an inner diameter of 31 mm as a mold. The beaker wall was insulated with rubber foam. The polymer solution at 80°C was poured into the beaker and the top was quickly insulated. The beaker was quenched at −20°C or −80°C with the bottom surface of the beaker directly contacting the cold surface. The insulating foam was then removed and the beaker was placed in 70% ethanol to extract the DMSO. The scaffold was then immersed in water and lyophilized. The resulting scaffolds had a diameter of 29 mm. Before evaluation the scaffold was cut to remove the bottom and top surfaces.

Scaffold Characterization

Scaffold morphology was examined with scanning electron microscopy (SEM). Transverse and longitudinal cross-sections (free of skin) were obtained relative to the direction of the applied thermal gradient by cutting the specimens after freezing in liquid nitrogen. Pore sizes were calculated from SEM micrographs using NIH image J software using three images for each scaffold type. Scaffold porosity was determined using a liquid displacement method previously described (6,27,28) that

was similar to that reported by Zhang and Ma (23) and Hsu *et al.* (29). Ethanol was used as the displacement liquid. A scaffold sample was immersed in a glass cylinder containing a known volume of ethanol (V_1). The sample was pressed to force air out of the scaffold until no further air bubbles were seen, allowing the ethanol to fill the pores. The total volume of ethanol and the ethanol-impregnated scaffold was recorded as V_2. The ethanol-impregnated scaffold was removed from the cylinder and the residual ethanol volume was recorded as V_3. The porosity (p) of the scaffold was determined by:

$$p = (V_1 - V_3)/(V_2 - V_3)$$

The tensile properties of the scaffolds were measured according to ASTM D638-98. Testing was conducted in an ATS testing machine equipped with a 5-lb load cell with a cross-head speed of 10 mm/min. For random scaffolds, the longitudinal direction of the conduit was tested (n=4). For scaffolds made with applied thermal gradients, both longitudinal (n=4) and transverse (n=4) directions were tested.

Scaffold Degradation

PU scaffold degradation studies were conducted in a 10-ml solution consisting of PBS (pH=7.4) with or without 0.3 mg/ml elastase (Sigma, type I, from porcine pancreas). Each scaffold (~50 mg, 9-mm diameter, and 6-mm thick) was immersed in the solution and was pressed to force the air out and to fill the pores with fluid. The degradation was conducted at 37°C in a water bath with the degradation solution exchanged every 7 days. At defined time points, samples were taken out, rinsed with water and dried in a vacuum oven for 3 days. The weight loss was calculated as:

$$\textit{Weight loss}(\%) = 100 \times (w_1 - w_2)/w_1$$

where w_1 and w_2 are the weights of scaffolds before and after degradation, respectively. The data for PU film degradation was used from a previous report (5) to compare degradation rates between the film and scaffold.

Muscle-Derived Stem Cell Seeding in Random and Oriented Pore Scaffolds

Mouse muscle-derived stem cells (MDSCs) were employed to evaluate the effect of scaffold pore structure on cell growth. MDSCs were isolated by the laboratory of Dr. Johnny Huard at the University of Pittsburgh using a pre-plating technique and have been shown to have the potential to differentiate into skeletal and smooth muscle cells and endothelial cells, among other cell types (30,31). Cells were expanded to between passages 10 and 15 by supplementing with culture medium containing DMEM and 10% fetal bovine serum (FBS). Both random and oriented scaffolds made from a 10% PU solution concentration and cooled at −80°C were evaluated. The scaffolds had been sterilized by immersion in 70% ethanol for 2 h, followed by five PBS rinses to extract the ethanol. Scaffolds were then placed in culture medium (DMEM supplemented with 10% FBS) for 12 h. A filtration seeding method was employed to seed MDSCs at a density of 3×10^6/ml into the scaffolds (6). The seeded constructs were then placed in a 12-well polystyrene tissue culture plate. After 24 h, the constructs were transferred into spinner flasks each filled with 100 ml culture medium and a rotation speed of 18 rpm. The culture medium was replaced twice a week. At 3 and 7 days, randomly selected constructs were taken out and evaluated for cell viability by MTT assay (6). For histological analysis, samples were frozen sectioned (15-μm thickness) after fixation in 10% formaldehyde. The sections were stained with hematoxylin and eosin (H & E).

Subcutaneous Implantation of Randomly Oriented Pore Scaffolds with and without Elastase Sensitivity

Adult female Lewis rats (Harlan Sprague Dawley, Indianapolis, IN, USA) weighing 200–250 g were used. The protocol followed National Institutes of Health (NIH) guidelines for animal care and was approved by the University of Pittsburgh Institutional Animal Care and Use Committee and Children's Hospital of Pittsburgh Animal Research Care Committee. The rats were anesthetized with an intramuscular injection of ketamine hydrochloride (22 mg/kg), followed by an intraperitoneal injection of sodium pentobarbital (30 mg/kg). The hair on the back of the rat was trimmed with an electrical clipper. Before skin incision, one dose of cefuroxime (100 mg/kg) as an antibiotic was administered intramuscularly for prophylaxis of surgical infection. The skin of the right back was cut with a 1.0-cm incision in each dorsal lumbar region, and a subcutaneous pocket was made. The scaffolds (6 mm in diameter and 500 μm in thickness) were placed in the pocket, using a 7–0 polypropylene with over-and-over peripheral sutures. Scaffolds made from a polymer concentration of 10% and quenching temperature −80°C were implanted (denoted as PU1080, n=8). Scaffolds made from a poly(ester urethane)urea synthesized with the same polymer soft (PCL) and hard (BDI) segments but chain extended with elastase insensitive putrescine instead of AAK were fabricated under the same conditions described above for randomly oriented scaffolds and were used as control (denoted as PEUU, n=8) (6). The skin was then closed with 4–0 polyglactin absorbable suture (Vicryl, Ethicon, Inc.) At 4 and 8 weeks post-implantation (n=4 for each group and each time-point), animals were sacrificed. After macroscopic photography of the material *in situ*, the material implant location was harvested and frozen in 2-methylbutane, which was pre-cooled in liquid nitrogen followed by sectioning, staining with H&E and histological assessment.

Statistical Methods

Data are expressed as mean ± standard deviation. Single-factor analysis of variance (ANOVA) was employed together with Neuman–Keuls post hoc testing for evaluations of differences between specific groups.

RESULTS

Fabrication of Randomly Oriented Porous Scaffolds

The synthesized PU had relatively high molecular weights with Mw 39,700 and Mn 22,000. PU films were observed to be highly flexible and strong possessing a tensile strength of 28±4 MPa and breaking strain of 830±80%. Figure 1 shows the cross-sectional morphologies of randomly

oriented porous scaffolds. Scaffold fabrication parameters such as solvent type, polymer solution concentration and quenching temperature were studied for their effect on pore morphology, pore size and porosity. When dissolving the same amount of PU in either dioxane or DMSO solvents, it was found that the viscosity of the dioxane solution was higher than that of the DMSO solution. Polymer solutions of 3 wt% were employed to fabricate scaffolds to investigate the effect of solvent type on scaffold morphology. In Fig. 1A it is seen that the scaffold made from a dioxane solution and cooled in −80°C had a mixture of small closed and open pores with nearly half of them being closed. Polymer fibers were spread across the pores. Scaffolds fabricated from dioxane and cooled at −20°C had larger, but still mostly closed pores (Fig. 1E). The presence of scattered polymer fibers was pronounced. At the same polymer concentration, scaffolds made from DMSO solutions exhibited open and interconnected pores (Fig. 1B and F). Pore interconnectivity was evidenced by the high scaffold porosities (greater than 85%) and the morphological evidence found in the electron micrographs. When the concentration and quenching temperature were the same, scaffolds fabricated from DMSO had larger pores and significantly higher porosity than those fabricated from dioxane (Table I).

Based on these observations, scaffolds for the rest of the study were fabricated using DMSO solutions. Figure 1 and Table I show that all of the DMSO based scaffolds possessed open and interconnected pores with mean pore sizes greater than 75 μm and porosities exceeding 86%. To study the effect of quenching temperature, two different temperatures (−20 and −80°C) were used to process the polymer. Scaffolds fabricated from 3% and 10% polymer concentrations at both temperatures displayed random morphology (Fig. 1B, D, F and H). When the PU concentration was 10%, a quenching temperature change from −80 to −20°C did not alter the mean pore size (Table I). When the PU concentration was 3%, pore sizes for scaffolds made at −20°C were larger than for those made at −80°C (Table I). When the PU concentration was 8%, scaffolds fabricated at −80°C had tubular pores (Fig. 1C) whereas scaffolds fabricated at −20°C possessed the more common random structure (Fig. 1G).

To examine the effect of polymer concentration on scaffold morphology, three different PU concentrations, 3%, 8% and 10%, were employed to fabricate scaffolds at −20 and

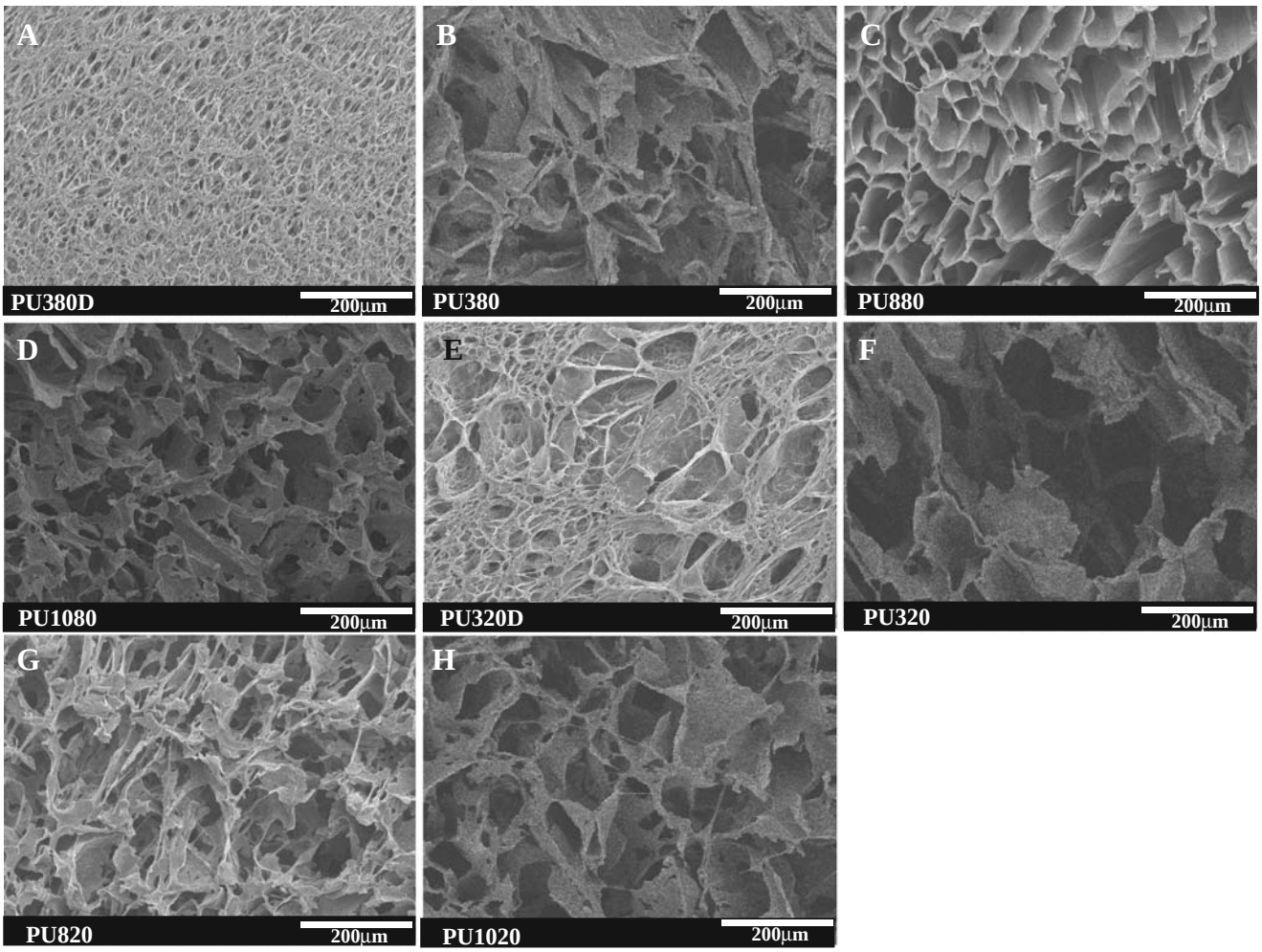

Fig. 1. Scaffolds fabricated under variable conditions that were not designed to induce oriented pore formation (abbreviations are those from Table I). **A** PU380D, **B** PU380, **C** PU880, **D** PU1080, **E** PU320D, **F** PU320, **G** PU820 and **H** PU1020. Scale bars are 200 um.

Table I. Scaffold Generation and Characterization (Without Thermal Gradients)

Polymer	Solvent	Concentration (*w*/*v*%)	Quenching temp. (°C)	Pore size (μm)	Pore size range (μm)	Porosity (%)
PU1080	DMSO	10	−80	75±62	31–135	87
PU1020	DMSO	10	−20	86±73	27–145	87
PU880	DMSO	8	−80	88±75	51–163	88
PU820	DMSO	8	−20	145±121	58–287	90
PU380	DMSO	3	−80	137±135	50–298	93
PU320	DMSO	3	−20	194±183	58–390	92
PU380D	Dioxane	3	−80	27±18	12–44	79
PU320D	Dioxane	3	−20	57±55	20–112	72

−80°C respectively. When the quenching temperature was −20°C, all of the scaffolds had a random pore structure and did not change observably with polymer concentration (Fig. 1F–H). However, the mean pore size decreased with an increase of polymer concentration (Table I). When the quenching temperature was −80°C, a polymer concentration increase from 3% to 8% decreased pore size. Further increases in polymer concentration did not change pore size significantly ($p>0.1$, Fig. 1B–D and Table I).

Fabrication of Scaffolds with Oriented Pore Structure

Scaffolds with oriented pore structures (oriented scaffolds) were fabricated by controlling heat transfer to favor one direction during the thermally induced phase separation process. Figure 2 shows cross-sectional morphologies of longitudinal and transverse directions in the resulting scaffolds, all of which showed an oriented parallel pore structure. All of the pores were observed to be open and displayed interconnections. The average pore sizes measured from the transverse direction of the scaffolds were greater than 88 μm and porosities exceeded 87% (Table II). When the quenching temperature was −20°C, scaffolds made from 8% and 10% polymer solution had more uniform pores than those made from a 5% PU solution (Fig. 2A–F). Pore sizes were larger than 120 μm for all of these scaffolds and were slightly decreased by increasing PU concentration from 5% to 10%. When the quenching temperature was −80°C, scaffolds also showed uniform pore morphology (Fig. 2G and H). When the PU concentration was 10%, comparing the pore sizes of scaffolds made at −20°C or −80°C quenching temperatures, it was found that scaffold made at −80°C had smaller pores (Table II).

Mechanical Properties

Figure 3 shows typical tensile stress-strain curves for a randomly oriented scaffold (PU1080), and for the longitudinal and transverse directions of an oriented scaffold (GPU1080), reflecting the anisotropic behavior of the latter. In Fig. 4 the tensile strengths and breaking strains of the PU scaffolds processed under conditions to favor random scaffolds are summarized. All of the scaffolds were flexible with breaking strains from 87% to 166%. Scaffolds possessed tensile strengths from 0.10 to 0.29 MPa except PU320, which had a markedly lower tensile strength of 0.04 MPa. For scaffolds fabricated at −80°C, increasing the PU solution concentration was associated with increased tensile strength ($p<0.05$), but not a significant effect on the breaking strain ($p>0.1$). For scaffolds fabricated at −20°C, increasing the PU concentration from 3% to 8% significantly increased tensile strength ($p<0.05$). However, the tensile strength did not change when the polymer concentration was increased from 8% to 10% ($p>0.05$). The same trend was found for breaking strain. At the same polymer concentration, the scaffolds processed at −20°C had lower tensile strengths and breaking strains than those made at −80°C.

Figure 5 summarizes the tensile properties of the scaffolds processed under thermal gradient conditions. All of the oriented scaffolds exhibited markedly different mechanical properties between the oriented (longitudinal) and non-oriented (transverse) directions with the direction of pore orientation possessing much higher tensile strengths and breaking strains ($p<0.01$). The oriented scaffolds had tensile strengths greater than 1.11 MPa in the longitudinal direction and less than 0.18 MPa in the transverse direction. Comparing scaffolds made from 10% PU and quenched at −20°C, the random scaffold had a tensile strength of 0.12 MPa (Fig. 4), while the oriented scaffold had tensile strength of 1.20 MPa in the longitudinal direction and 0.18 MPa in the transverse direction. The oriented scaffold PU1020 had over four times higher distensibility in the longitudinal direction than the transverse direction. For scaffolds fabricated at −20°C, the decrease in polymer concentration from 10% to 8% did not change tensile strength significantly in both longitudinal and transverse directions ($p>0.05$), while the breaking strain increased significantly in both directions ($p<0.05$; Fig. 5). At the same 10% PU concentration, a quenching temperature decrease from −20°C to −80°C increased the tensile strength and breaking strain in the longitudinal direction ($p<0.01$) and did not change these parameters in the transverse direction ($p>0.05$; Fig. 5).

Scaffold Degradation

Figure 6 shows the degradation curves of PU1080 scaffolds in PBS solution at 37°C with or without elastase addition. Scaffolds exhibited progressive mass loss over the 8-week period. The presence of elastase significantly increased scaffold mass loss. Scaffolds exhibited higher mass loss than historical data from PU films in PBS with elastase. After 56 days of degradation in PBS, the film (historical data) and scaffold had similar weight loss (11.9% for film and 12.7% for scaffold, $p>0.1$). However, in PBS with elastase the scaffold showed higher weight loss than the film (41.6% and 27.1% respectively, $p<0.02$) (5).

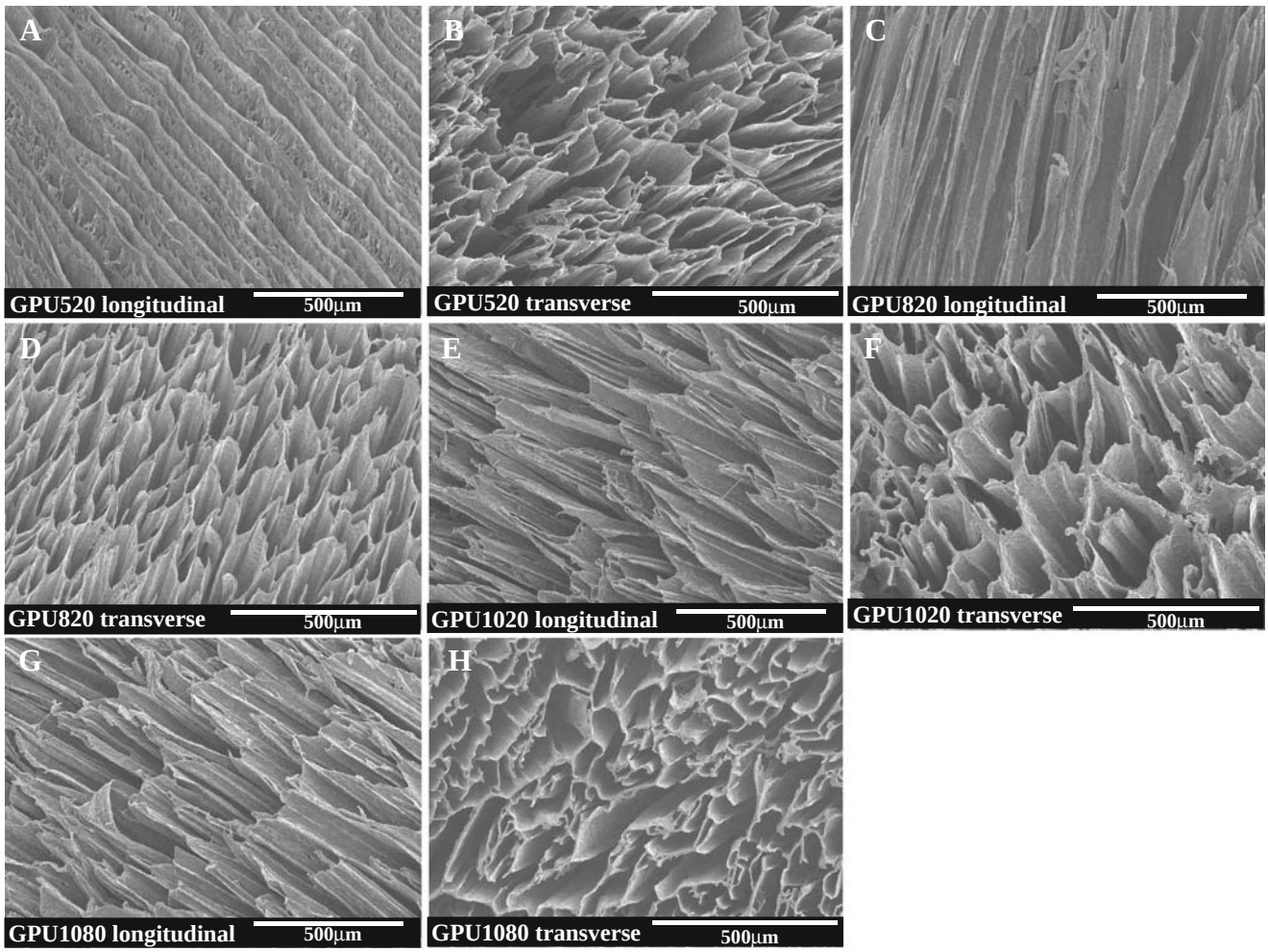

Fig. 2. Scaffolds fabricated under variable conditions with thermal gradients that were designed to induce oriented pore formation (abbreviations are those from Table II). **A** GPU520 longitudinal, **B** GPU520 transverse, **C** GPU820 longitudinal, **D** GPU820 transverse, **E** GPU1020 longitudinal, **F** GPU1020 transverse, **G** GPU1080 longitudinal, and **H** GPU1080 transverse. Scale bars are 500 um.

Muscle Derived Stem Cell Growth: Effect of Oriented Pores

Muscle derived stem cells were seeded in both random (PU1080) and oriented (GPU1080) scaffolds to investigate the effect of pore morphology on cell growth. Figure 7 shows the relative cell number in the scaffolds after 3 and 7 days of culture with numbers increasing for both scaffolds during the 7 days of culture. At each time point, the cell number in oriented scaffolds was significantly higher than that of the random scaffolds ($p<0.05$). H & E staining at 7 days (Fig. 8) qualitatively confirmed this result with higher cell densities apparent in the oriented scaffold.

Subcutaneous Implantation of Randomly Oriented Scaffolds

Elastase sensitive PU1080 scaffolds and elastase insensitive PEUU scaffolds were implanted in rat subcutaneous tissue for 4 and 8 weeks to investigate *in vivo* PU scaffold degradation and tissue ingrowth. No infection was observed in the skin and subcutaneous tissues during the postoperative course or at the time of explant. Figure 9 shows the representative macroscopic images of the scaffolds 4 and 8 weeks following surgery. For the elastase insensitive PEUU scaffold, its surface was covered with connective tissue at both time-points (Fig. 9A and B). At 4 weeks, a large amount of the scaffold remained and the

Table II. Scaffold Generation and Characterization (with Thermal Gradients)

Polymer	Polymer conc. (*w*/*v*%)	Quenching temp. (°C)	Pore size[a] (μm)	Pore size range[a] (μm)	Porosity (%)
GPU520	5	−20	139±131	63–290	88
GPU820	8	−20	129±103	74–231	90
GPU1020	10	−20	121±44	50–228	88
GPU1080	10	−80	89±27	49–117	91

[a] Pore sizes were measured from electron micrographs for the transverse scaffold direction.

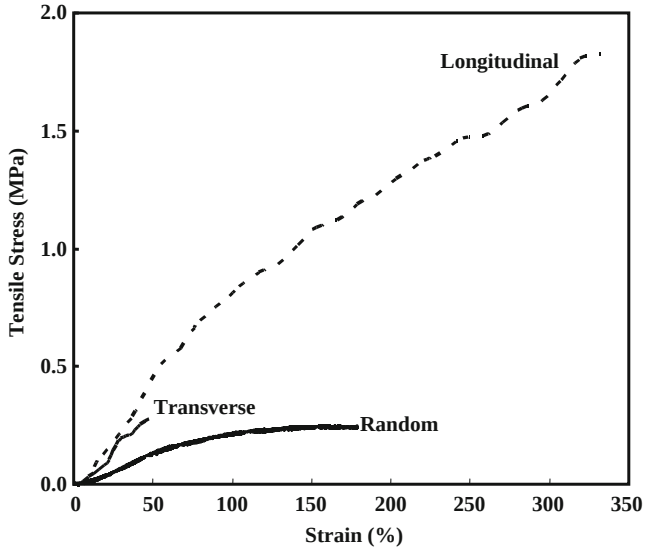

Fig. 3. Typical stress–strain curves for the random scaffold PU1080, and the longitudinal and transverse directions of the oriented scaffold GPU1080.

original circular shape was maintained, while at 8 weeks, a substantial fraction of the PEUU was degraded. For elastase-sensitive PU1080 scaffolds (Fig. 9C and D), almost all of the scaffold was degraded at 4 weeks and complete degradation had occurred by 8 weeks. In Fig. 10 histological cross sections of the implanted scaffolds and nearby tissue are presented. At 4 weeks, the PEUU scaffold had cellular ingrowth consistent with an expected infiltrate of macrophages and fibroblasts (Fig. 10A). At 8 weeks, the PEUU scaffold was largely absorbed, but a cellular infiltrate of putative macrophages remained accumulated at the implant site (Fig. 10B). For the PU1080 scaffold, a cellular infiltrate around the remaining material was seen at 4 weeks (Fig. 10C), by 8 weeks the infiltrate had dissipated and minimal evidence remained of the implant (Fig. 10D).

DISCUSSION

A significant amount of work has been reported in the literature in recent years in the area of enzymatically responsive materials (32). In the tissue engineering area, much of this work has focused on the development of hydrogels crosslinked with enzyme specific peptide sequences. West and Hubbell first reported the generation of photopolymerizable poly(ethylene)glycol hydrogels crosslinked with enzymatically labile peptide sequences, including collagenase and plasmin responsive elements (33). A subsequent report by West and colleagues showed that a poly (alanine)–lysine sequence introduced elastase sensitivity in these hydrogels (34). Other hydrogels have similarly been crosslinked with enzymatically labile peptides, including thermoresponsive polymers (35) and most recently dextran (36). A feature of much of this hydrogel work is the ability to orchestrate cell adhesion onto or migration within the relatively non-adhesive hydrogels by covalently attaching specific adhesion peptide sequences. These types of hydrogels have allowed investigation of three-dimensional cell migration dependent on cell-initiated gel lysis (37,38) and, recently, on the effect of enveloping hydrogel properties on cardiogenitor cell differentiation (39).

In this report we have focused on an enzymatically labile thermoplastic elastomer (5) and have sought to capitalize on the solvent processing options that are available with a non-crosslinked system. Our general objective, to fabricate 3D microporous scaffolds suitable for soft tissue engineering from an elastase sensitive polyurethane, was met by appropriate manipulation of processing parameters in the thermally induced phase separation technique. Scaffold properties were dependent upon the solvent type, quenching temperature, polymer solution concentration and heat transfer direction. When dioxane was used as a solvent, the polymer solution was highly viscous, even at a polymer concentration of 3% the resulting scaffolds had a relatively high number of closed pores. This effect was probably due to high viscosity

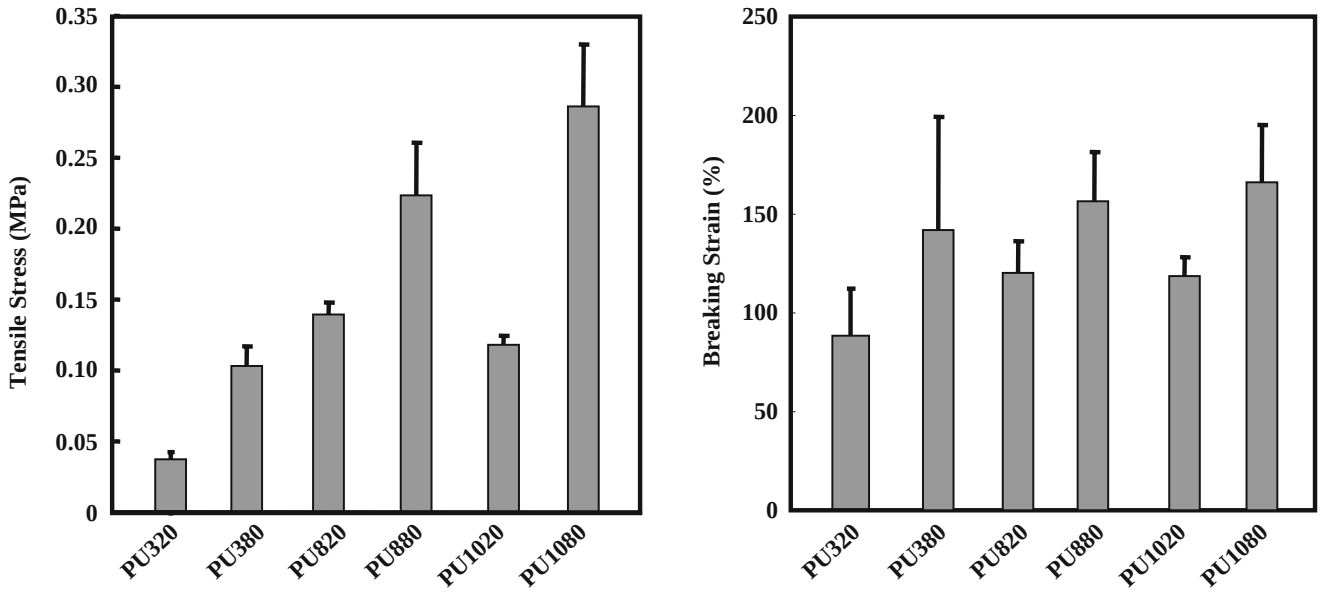

Fig. 4. Mechanical properties of random scaffolds.

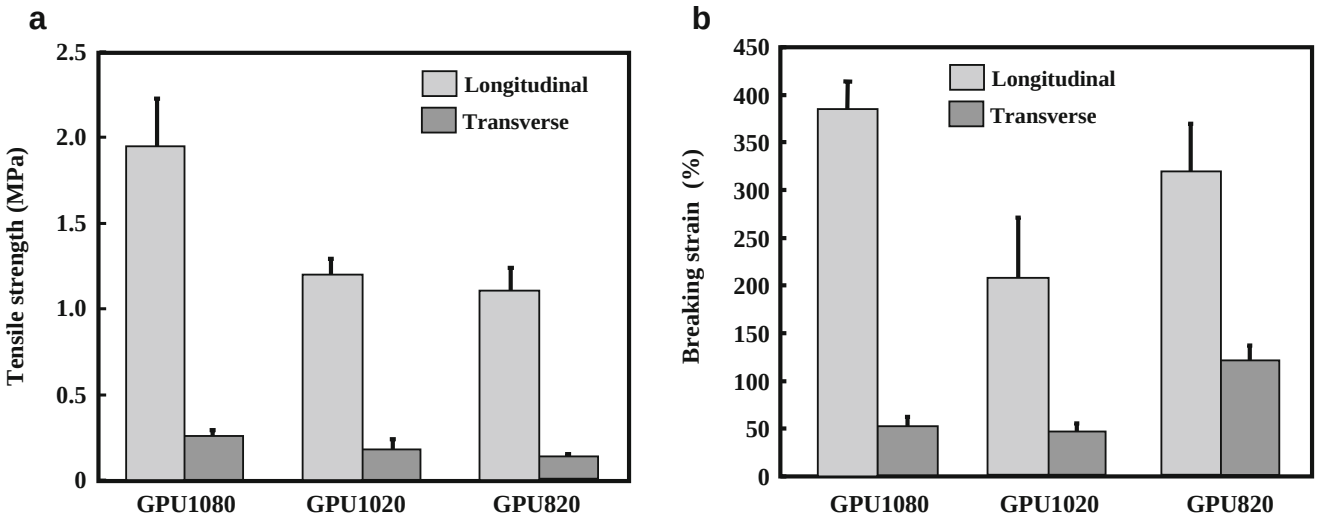

Fig. 5. Mechanical properties of oriented scaffolds. *Left* Effect of polymer concentration; *right* effect of quenching temperature.

hindering phase separation between dioxane and the polyurethane. A similar phenomenon was found by Spaans *et al.* (40) where only a thin layer of porous scaffolds could be obtained when using dioxane to process polyurethaneurea scaffolds. We thus modified the polymer/solvent system by replacing dioxane with DMSO and were able to generate scaffolds that displayed open and interconnected pores (Figs. 1 and 2). DMSO was chosen because of its high melting temperature (18.4°C). Moreover, DMSO has relatively low toxicity and is used for cell preservation.

The quenching temperature was found to affect scaffold morphology in a predictable manner. At the same PU concentration, increasing the quenching temperature increased average pore size (Tables I and II). This was controlled by DMSO crystallization kinetics. At a lower quenching temperature, the cooling rate was faster, leading to formation of a large number of nucleation sites that grew at a faster rate. This resulted in small crystals, which after DMSO extraction with ethanol, yielded small pores. At a higher quenching temperature, the cooling rate was slower, fewer nucleation sites were formed that grew at a slower rate, and the larger DMSO crystals left behind larger pores.

Figures 1 and 2, and Tables I and II show that the PU solution concentration affected pore morphology and size. Generally, increasing the PU concentration decreased pore size. This could be attributed to the effect of polymer solution viscosity on DMSO crystallization. At higher PU concentrations, the solutions had higher viscosity, which limited the growth of DMSO crystals to form larger pores. More polymer molecules in the higher concentration solution would also hinder DMSO molecular aggregation. It was found in Fig. 1

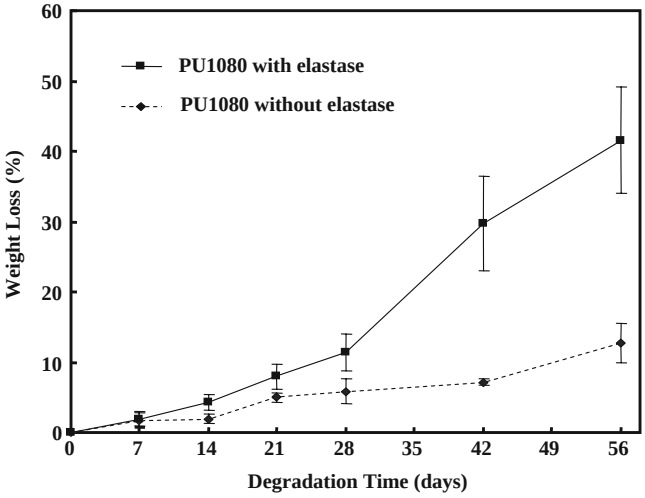

Fig. 6. Weight loss of PU1080 scaffolds in PBS with or without elastase.

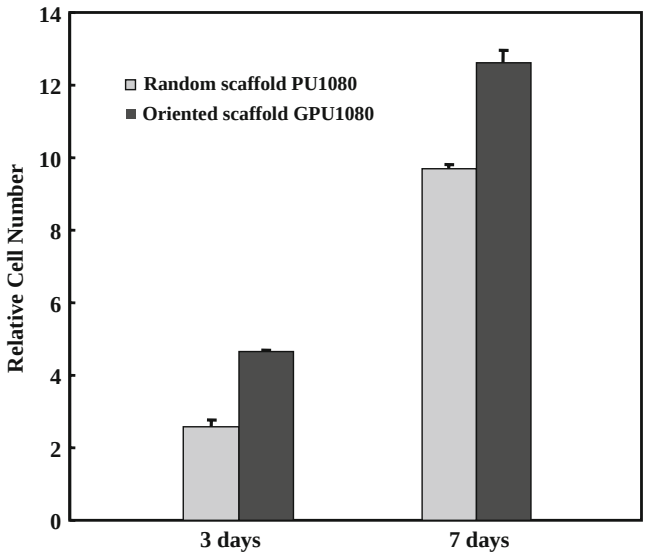

Fig. 7. Relative number of muscle derived stem cell in random (PU1080) and orientated (GPU1080) scaffolds after 3 and 7 days of culture. The cell number in oriented scaffolds was higher than random scaffolds at both time points ($p<0.05$). Oriented scaffolds cut transversely were used for cell culture.

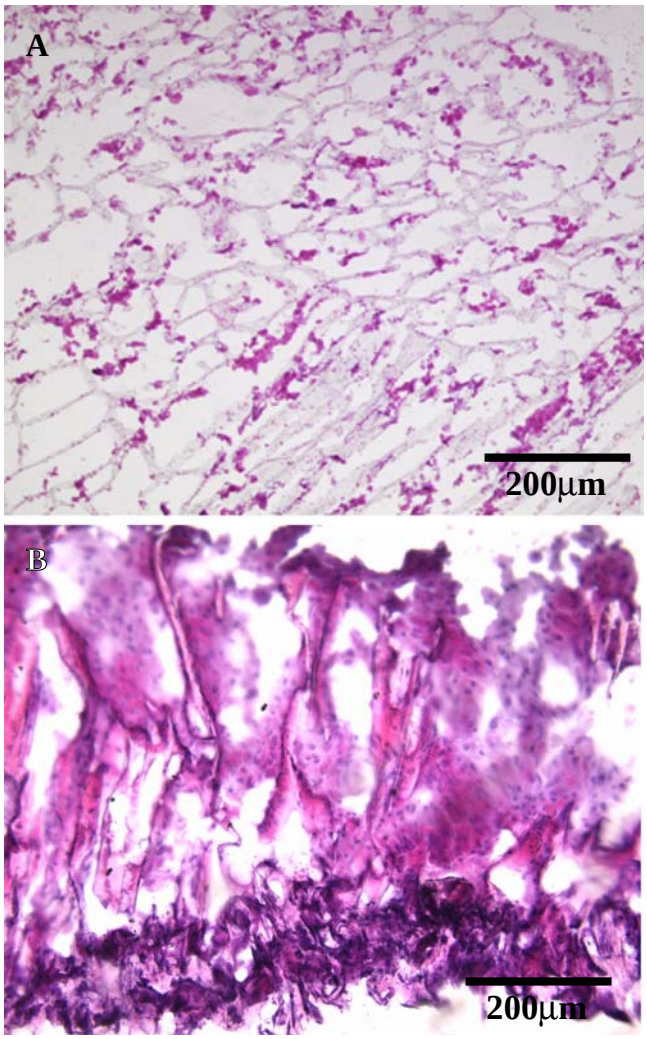

Fig. 8. H & E staining of random PU1080 (**A**) and oriented GPU1080 (**B**) scaffolds after 7 days of culture with muscle derived stem cells. Oriented scaffolds cut transversely were used for cell culture.

that at −80°C, the scaffold fabricated from 8% PU solution exhibited tubular like morphology, whereas scaffolds made from 3% and 10% PU had random morphology. This was also observed for other polyurethane elastomers that we have developed previously and may be attributed to the effect of solution viscosity on DMSO crystallization kinetics and crystal growth direction (6). Of note, in Fig. 1G where the scaffold was fabricated at the same PU concentration but quenched at −20°C, the tubular morphology was not found.

In an effort to obtain oriented scaffolds with various pore sizes, and to control the tubular morphology more efficiently, we chose to fabricate oriented scaffolds by controlling the heat transfer direction during the thermally induced phase separation process. When the mold without insulation was used, the resulting scaffolds had random morphology, whereas using the insulated mold with only one direction for heat transfer yielded the oriented morphology. This method of fabrication of oriented scaffolds is similar to previous reports (24,25). In this approach, DMSO crystals grow in the direction of the heat transfer and form aligned crystal rods. All of the oriented scaffolds had pore sizes ranging from 49 to 239 μm in the transverse direction and porosities higher than 87%. The pore size in these scaffolds was similarly dependent upon polymer concentration and quenching temperature. Scaffolds fabricated from higher PU concentrations had smaller pores than those from lower concentrations, and quenching at −20°C yielded larger pores than quenching at −80°C.

The random scaffolds were flexible and had uniform mechanical properties with tensile strengths ranging from 40 to 290 kPa and breaking strains from 87% to 166% (Fig. 4). The breaking strain was comparable to that of the rat heart (about 75%) and the tensile strength was close to or higher than that of the rat heart (approximately 40 kPa) (41). The general similarities in these tensile properties to that of the rat heart would be attractive in cardiac wall tissue engineering. Scaffolds made from a non-elastase sensitive poly(ester urethane)urea with similar mechanical properties have shown promising initial results in rat cardiac placement (42,43). Other soft tissue engineering applications such as skeletal muscle repair, blood vessel replacement and genitourinary applications would also seem amenable to the mechanical properties exhibited. Placement of a cell-laden scaffold, or scaffold alone into these tissue beds could provide for better mechanical coupling, without stress shielding, to these active tissues using this polymer and processing approach. Earlier work by Woodhouse and colleagues has similarly developed enzymatically sensitive polyurethanes by utilizing a phenylalanine diester chain extender and a polyester soft segment (44,45). This chain extender was shown to introduce chymotrypsin and, to a lesser extent, trypsin, sensitivity. A recent report from this group has demonstrated the ability to form this polyurethane into scaffolds using electrospinning and TIPS, with the latter resulting in porosities up to 36%. These scaffolds were shown to support seeded cardiomyocytes derived from murine embryonic stem cells *in vitro* as a step towards cardiac tissue engineering applications (46).

The oriented PU scaffolds had anisotropic mechanical properties with the longitudinal direction possessing significantly higher tensile strengths and breaking strains than the transverse direction. (Figs. 3 and 5) The transverse direction had similar tensile strengths to the randomly oriented scaffolds. (Figs. 4 and 5) For randomly oriented scaffolds, mechanical properties were dependent upon the pore structure, polymer concentration and quenching temperature. The tensile strength increased with increased PU solution concentration and decreased quenching temperature. Both trends can be attributed to an increased polymer density associated with smaller pores and decreased porosity. For oriented scaffolds, the tensile strength was mainly dependent on the quenching temperature, whereas polymer concentration change did not alter tensile strength in the longitudinal or transverse directions significantly. This effect can also be attributed to pore size changes where a PU concentration change from 10% to 8% did not change pore size significantly, but a decrease in quenching temperature significantly increased pore size. (Table II) Further exploration of the design space in terms of these processing parameters would likely yield similar effects to the random scaffolds where increased porosity or loss of mass in a given direction reduces tensile strength.

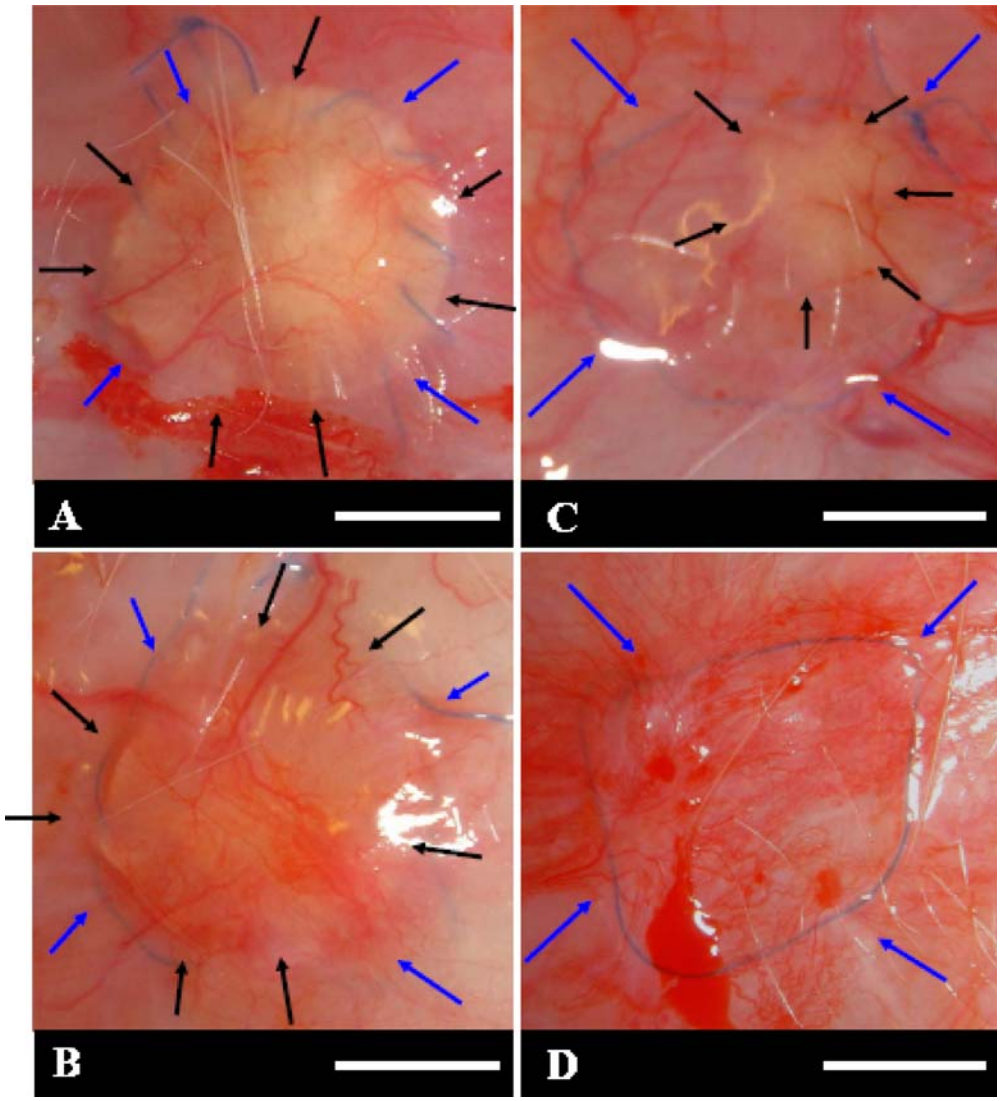

Fig. 9. Overview of subcutaneous implantation of PEUU scaffolds (**A** and **B**) and PU1080 scaffolds (**C** and **D**) after 4 (**A** and **C**) and 8 (**B** and **D**) weeks of implantation. *Blue* and *black arrows* denote sutures and scaffold edge respectively.

We have demonstrated in our initial description of the elastase sensitive polyurethane that the polymer used for this study possesses two primary degradation mechanisms, hydrolysis and elastase-dependent cleavage (5). For a 2D PU film, degradation in elastase was significantly faster than in PBS. Figure 6 shows similarly that mass loss for PU scaffolds with elastase in the buffer was markedly faster than for scaffolds when no elastase was present. The PU scaffold mass loss in elastase buffer was significantly higher than for PU films, an effect attributed to the markedly higher surface area of the scaffolds, allowing more water and/or elastase access to the surface to degrade the polymer. Our previous study showed that a polyurethane using elastase sensitive AAK as a chain extender had a significantly faster mass loss than a polyurethane using elastase insensitive putrescine as the chain extender in an elastase buffer (5). In contrast, in buffer without elastase, the 56-day mass loss for the corresponding scaffolds fabricated under the same conditions did not differ significantly (12.7±2.8 for AAK chain extended *versus* 15.3± 1.2 for putrescine chain extended) (6). Subcutaneous implantation results in rats seen in Figs. 9 and 10 demonstrated that AAK chain extended scaffolds had much faster *in vivo* mass loss than putrescine chain extended scaffolds. Although direct quantification of this phenomenon is difficult, the trends at 4 and 8 weeks were pronounced. It was found that the scaffold with both elastase and hydrolytic degradation mechanisms was resorbed at a faster rate than for the scaffold with only hydrolytic degradation mechanisms. The most direct interpretation of these *in vivo* data is that macrophages recruited to the implantation site and participating in the foreign body response are secreting elastase, which is participating to more rapidly degrade the AAK containing scaffolds. In our previous report on PU films, we showed that collagenase did not act upon the AAK sequence in short time periods, in marked contrast to elastase (5), but it is possible that several other enzymes are acting in a pronounced manner to degrade the PU at the peptide segments in the backbone. It is also possible that introduction of the peptide sequence, and not

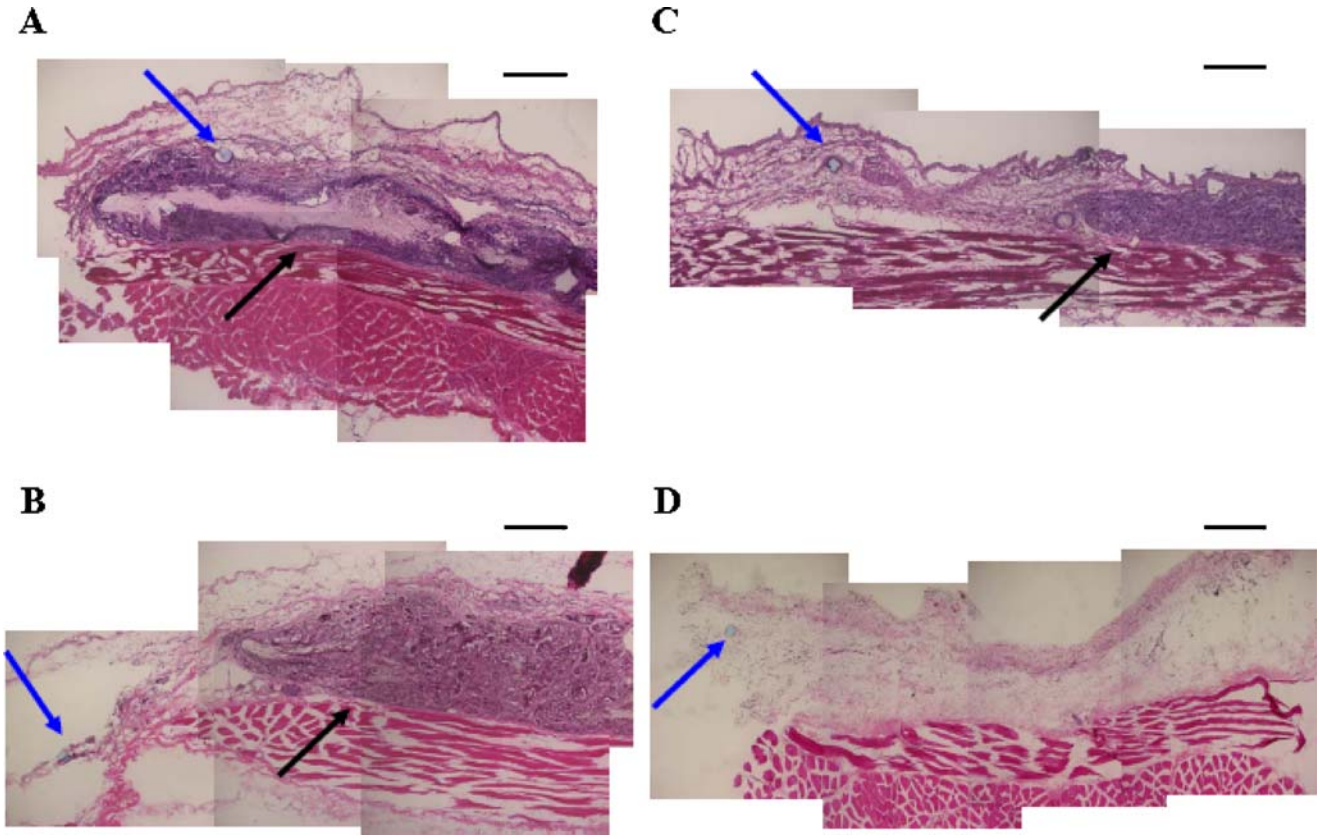

Fig. 10. H & E staining of PEUU scaffolds (**A** and **B**) and PU1080 scaffolds (**C** and **D**) after 4 (**A** and **C**) and 8 (**B** and **D**) weeks of implantation. *Blue* and *black arrows* denote sutures and scaffold edge respectively.

AAK specifically, is increasing lability of the polymer backbone *in vivo* to a variety of enzymes or differentially impacting macrophage behavior (47).

The *in vivo* results were performed in the absence of cell seeding or prior *in vitro* culture. To examine the potential for these scaffolds to support cells relevant for soft tissue engineering, muscle derived stem cells were employed to evaluate scaffold cytocompatibility and compare cell growth in random and oriented scaffolds. It was found that significantly higher cell densities could be achieved in the oriented *versus* random pore morphologies with *in vitro* culture (Figs. 7 and 8). This phenomenon may have been due to the less tortuous pores in the oriented scaffolds enabling more efficient oxygen and nutrient diffusion or potentially due to improved cell seeding efficiency with the oriented scaffolds. A limitation of these results is that we did not quantify cell numbers in the early period following cell seeding to differentiate these effects. The use of muscle-derived stem cells is of particular relevance to soft tissue engineering, since these cells have previously been shown to differentiate into skeletal muscle, endothelial cells, smooth muscle cells, and to have beneficial effects upon injection to treat urinary incontinence (30,48). These cells have also been injected into myocardial infarcts and have been demonstrated to provide benefit, although not by directly differentiating into cardiomyocytes (31,49). There is thus not evidence that cardiac wall could be tissue engineered with these cells *in vivo*, but that placement of these cells on the infarct region in an appropriately elastic scaffold might have benefit.

As a first level investigation the results demonstrate the cytocompatibility of the random and aligned PU scaffolds for various applications and suggest advantages for the oriented scaffolds in supporting cell growth. Longer term *in vitro* culture in bioreactor systems with imposed mechanical training followed by assessment of cellular alignment and cell phenotype as a function of scaffold architecture would be logical next steps to pursue with these materials. In addition, exploration of the effect of oriented pore structures on *in vivo* results would be of interest. The application of randomly oriented porous scaffolds made from hydrolytically labile, but not elastase sensitive, polyurethanes has been investigated in small animal models for pediatric and adult cardiac disease (42,43). The performance of an elastase sensitive polyurethane or the use of oriented pore structures in these experiments might provide advantages in altering the healing response. One could also develop alternative polyurethanes that incorporate peptide sequences specific for other enzymes and employ these materials or create blends with processing to achieve a synthetic scaffold with multiple enzyme responsiveness. This would still be far from the native extracellular matrix remodeling response, but such materials might provide altered healing depending upon the enzymatic activity specific to the site of implantation.

CONCLUSIONS

An elastase sensitive polyurethane was processed into microporous scaffolds having both random and oriented pore

structures. The scaffolds were flexible and the mechanical properties were dependent on the pore morphology, polymer concentration and quenching temperature. Oriented pore scaffolds demonstrated pronounced mechanical anisotropy and appeared to better support cell growth *in vitro* than random scaffolds. The scaffolds were sensitive to elastase *in vitro* and exhibited faster degradation rates *in vivo* when compared to control polyurethanes. These scaffolds, which are responsive to a naturally occurring tissue remodeling process in addition to simple hydrolysis may find further use in the engineering of mechanically active soft tissues.

ACKNOWLEDGEMENT

This work was supported by the National Institutes of Health (grant no. HL069368). We are grateful to the laboratory of Dr. Johnny Huard at the University of Pittsburgh for their provision of mouse muscle derived stem cells.

REFERENCES

1. L. E. Niklason, J. Gao, W. M. Abbott, K. K. Hirschi, S. Houser, R. Marini, and R. Langer. Functional arteries grown *in vitro*. *Science*. **284**:489–493 (1999).
2. S. P. Hoerstrup, G. Zund, R. Sodian, A. M. Schnell, J. Grunenfelder, and M. I. Turina. Tissue engineering of small caliber vascular grafts. *Eur. J. Cardiothorac. Surg*. **20**:164–169 (2001).
3. A. Tiwari, H. J. Salacinski, G. Punshon, G. Hamilton, and A. M. Seifalian. Development of a hybrid cardiovascular graft using a tissue engineering approach. *FASEB J*. **16**:791–796 (2002).
4. F. Opitz, K. Schenke-Layland, W. Richter, D. P. Martin, I. Degenkolbe, T. Wahlers, and U. A. Stock. Tissue engineering of ovine aortic blood vessel substitutes using applied shear stress and enzymatically derived vascular smooth muscle cells. *Ann. Biomed. Eng*. **32**:212–222 (2004).
5. J. Guan, and W. R. Wagner. Synthesis, characterization and cytocompatibility of polyurethaneurea elastomers with designed elastase sensitivity. *Biomacromolecules*. **6**:2833–2842 (2005).
6. J. Guan, K. L. Fujimoto, M. S. Sacks, and W. R. Wagner. Preparation and characterization of highly porous, biodegradable polyurethane scaffolds for soft tissue applications. *Biomaterials*. **26**:3961–3971 (2005).
7. J. Guan, M. S. Sacks, E. J. Beckman, and W. R. Wagner. Biodegradable poly(ether ester urethane)urea elastomers based on poly(ether ester) triblock copolymers and putrescine: synthesis, characterization and cytocompatibility. *Biomaterials*. **25**:85–96 (2004).
8. J. Guan, M. S. Sacks, E. J. Beckman, and W. R. Wagner. Synthesis, characterization, and cytocompatibility of elastomeric, biodegradable poly(ester-urethane)ureas based on poly(caprolactone) and putrescine. *J. Biomed. Mater. Res*. **61**:493–503 (2002).
9. J. D. Fromstein, and K. A. Woodhouse. Elastomeric biodegradable polyurethane blends for soft tissue application. *J. Biomater. Sci. Polymer. Ed*. **13**:391–406 (2002).
10. L. Tatai, T. G. Moore, R. Adhikari, F. Malherbe, R. Jayasekara, I. Griffiths, and P. A. Gunatillake. Thermoplastic biodegradable polyurethanes: the effect of chain extender structure on properties and in-vitro degradation. *Biomaterials*. **28**:5407–5417 (2007).
11. K. D. Kavlock, T. W. Pechar, J. O. Hollinger, S. A. Guelcher, and A. S. Goldstein. Synthesis and characterization of segmented poly(esterurethane urea) elastomers for bone tissue engineering. *Acta Biomater*. **3**:475–484 (2007).
12. Q. Z. Chen, A. Bismarck, U. Hansen, S. Junaid, M. Q. Tran, S. E. Harding, N. N. Ali, and A. R. Boccaccini. Characterisation of a soft elastomer poly(glycerol sebacate) designed to match the mechanical properties of myocardial tissue. *Biomaterials*. **29**:47–57 (2008).
13. Y. Wang, G. Ameer, B. Sheppard, and R. Langer. A tough biodegradable elastomer. *Nat. Biotechnol*. **20**:602–606 (2002).
14. J. Yang, A. Webb, and G. A. Ameer. Novel citric acid-based biodegradable elastomers for tissue engineering. *Adv. Mater*. **16**:511–516 (2004).
15. R. Murugan, and S. Ramakrishna. Design strategies of tissue engineering scaffolds with controlled fiber orientation. *Tissue Eng*. **13**:1845–1866 (2007).
16. Q. P. Pham, U. Sharma, and A. G. Mikos. Electrospinning of polymeric nanofibers for tissue engineering applications: a review. *Tissue Eng*. **12**:1197–1211 (2006).
17. T. Courtney, M. S. Sacks, J. J. Stankus, J. Guan, and W. R. Wagner. Design and analysis of tissue engineering scaffolds that mimic soft tissue mechanical anisotropy. *Biomaterials*. **27**:3631–3638 (2006).
18. K. Fujimoto, M. Minato, S. Miyamoto, T. Kaneko, H. Kikuchi, K. Sakai, M. Okada, and Y. Ikada. Porous polyurethane tubes as vascular graft. *J. Appl. Biomater*. **4**:347–354 (1993).
19. R. P. Kowligi, W. W. von Maltzahn, and R. C. Eberhart. Fabrication and characterization of small-diameter vascular prostheses. *J. Biomed. Mater. Res*. **22**:245–256 (1988).
20. K. Doi, Y. Nakayama, and T. Matsuda. Novel compliant and tissue permeable microporous polyurethane vascular prosthesis fabricated using an excimer laser ablation technique. *J. Biomed. Mater. Res*. **31**:27–33 (1996).
21. S. Q. Liu, and M. Kodama. Porous polyurethane vascular prostheses with variable compliances. *J. Biomed. Mater. Res*. **26**:1489–1494 (1992).
22. Y. S. Nam, and T. G. Park. Porous biodegradable polymeric scaffolds prepared by thermally induced phase separation. *J. Biomed. Mater. Res*. **47**:8–17 (1999).
23. R. Y. Zhang, and P. X. Ma. Poly(a-hydroxyl acids)/hydroxyapatite porous composites for bone-tissue engineering. I. Preparation and morphology. *J. Biomed. Mater. Res*. **44**:446–455 (1999).
24. P. X. Ma, and R. Y. Zhang. Microtubular architecture of biodegradable polymer scaffolds. *J. Biomed. Mater. Res*. **56**:469–477 (2001).
25. F. Yang, X. Qu, W. J. Cui, J. Z. Bei, F. Y. Yu, S. B. Lu, and S. G. Wang. Manufacturing and morphology structure of polylactide-type microtubules orientation-structured scaffolds. *Biomaterials*. **27**:4923–4933 (2006).
26. A. S. Rowlands, S. A. Lim, D. Martin, and J. J. Cooper-White. Polyurethane/poly(lactic-co-glycolic) acid composite scaffolds fabricated by thermally induced phase separation. *Biomaterials*. **28**:2109–2121 (2007).
27. J. Guan, J. J. Stankus, and W. R. Wagner. Biodegradable elastomeric scaffolds with basic fibroblast growth factor release. *J. Control. Release*. **120**:70–78 (2007).
28. J. Guan, J. J. Stankus, and W. R. Wagner. Development of composite porous scaffolds based on collagen and biodegradable poly(ester urethane)urea. *Cell Transplant*. **15**:S17–S27 (2006).
29. Y. Y. Hsu, J. D. Gresser, D. J. Trantolo, C. M. Lyons, P. R. Gangadharam, and D. L. Wise. Effect of polymer foam morphology and density on kinetics of *in vitro* controlled release of isoniazid from compressed foam matrices. *J. Biomed. Mater. Res*. **35**:107–116 (1997).
30. Z. Qu-Petersen, B. Deasy, R. Jankowski, M. Ikezawa, J. Cummins, R. Pruchnic, J. Mytinger, B. Cao, C. Gates, A. Wernig, and J. Huard. Identification of a novel population of muscle stem cells in mice: potential for muscle regeneration. *J. Cell Biol*. **157**:851–864 (2002).
31. H. Oshima, T. R. Payne, K. L. Urish, T. Sakai, Y. Ling, B. Gharaibeh, K. Tobita, B. B. Keller, J. H. Cummins, and J. Huard. Differential myocardial infarct repair with muscle stem cells compared to myoblasts. *Molec. Ther*. **12**:1130–1141 (2005).
32. R. V. Ulijn. Enzyme-responsive materials: a new class of smart biomaterials. *J. Mater. Chem*. **16**:2217–2225 (2006).
33. J. L. West, and J. A. Hubbell. Polymeric biomaterials with degradation sites for proteases involved in cell migration. *Macromolecules*. **32**:241–244 (1999).
34. B. K. Mann, A. S. Gobin, A. T. Tsai, R. H. Schmedlen, and J. L. West. Smooth muscle cell growth in photopolymerized hydrogels with cell adhesive and proteolytically degradable domains: synthetic ECM analogs for tissue engineering. *Biomaterials*. **22**:3045–3051 (2001).

35. S. Kim, E. H Chung, M. Gilbert, and K. E. Healy. Synthetic MMP-13 degradable ECMs based on poly(*N*-isopropylacrylamide-co-acrylic acid) semi-interpenetrating polymer networks. I. Degradation and cell migration. *J. Biomed. Mater. Res. A*. **75**:73–88 (2005).
36. S. G. Lévesque, and M. S. Shoichet. Synthesis of enzyme-degradable, peptide-cross-linked dextran hydrogels. *Bioconjug. Chem*. **18**:874–885 (2007).
37. G. P. Raeber, M. P. Lutolf, and J. A. Hubbell. Mechanisms of 3-D migration and matrix remodeling of fibroblasts within artificial ECMs. *Acta Biomater*. **3**:615–629 (2007).
38. A. S. Gobin, and J. L. West. Cell migration through defined, synthetic extracellular matrix analogs. *FASEB J*. **16**:751–753 (2002).
39. T. P. Kraehenbuehl, P. Zammaretti, A. J. Van der Vlies, R. G. Schoenmakers, M. P. Lutolf, M. E. Jaconi, and J. A. Hubbell. Three-dimensional extracellular matrix-directed cardioprogenitor differentiation: systematic modulation of a synthetic cell-responsive PEG–hydrogel. *Biomaterials*. **29**:2757–2766 (2008).
40. C. J. Spaans, J. H. de Groot, F. G. Dekens, and A. J. Pennings. High molecular weight polyurethanes and a polyurethane urea based on 1,4-butanediisocyanate. *Polym. Bull*. **41**:131–138 (1998).
41. J. Boublik, H. Park, M. Radisic, E. Tognana, F. Chen, M. Pei, G. Vunjak-Novakovic, and L. E. Freed. Mechanical properties and remodeling of hybrid cardiac constructs made from heart cells, fibrin, and biodegradable, elastomeric knitted fabric. *Tissue Eng*. **11**:1122–1132 (2005).
42. K. L. Fujimoto, J. Guan, H. Oshima, T. Sakai, and W. R. Wagner. *In vivo* evaluation of a porous, elastic, biodegradable patch for reconstructive cardiac procedures. *Ann. Thorac. Surg*. **83**:648–654 (2007).
43. K. L. Fujimoto, K. Tobita, W. D. Merryman, J. Guan, N. Momoi, D. B. Stolz, M. S. Sacks, B. B. Keller, and W. R. Wagner. An elastic, biodegradable cardiac patch induces contractile smooth muscle and improves cardiac remodeling and function in subacute myocardial infarction. *J. Am. Coll. Cardiol*. **49**:2292–2300 (2007).
44. G. A. Skarja, and K. A. Woodhouse. Synthesis and characterization of degradable polyurethane elastomers containing and amino acid-based chain extender. *J. Biomater. Sci. Polym. Ed*. **9**:271–295 (1998).
45. G. A. Skarja, and K.A. Woodhouse. *In vitro* degradation and erosion of degradable, segmented polyurethanes containing an amino acid-based chain extender. *J. Biomater. Sci. Polym. Ed*. **12**:851–873 (2001).
46. J. D. Fromstein, P. W. Zandstra, C. Alperin, D. Rockwood, J. F. Rabolt, and K.A. Woodhouse. Seeding bioreactor-produced embryonic stem cell-derived cardiomyocytes on different porous, degradable, polyurethane scaffolds reveals the effect of scaffold architecture on cell morphology. *Tissue Eng. Part A*. **14**:369–378 (2008).
47. D. L. Dinnes, J. P. Santerre, and R. S. Labow. Influence of biodegradable and non-biodegradable material surfaces on the differentiation of human monocyte-derived macrophages. *Differentiation*. **76**:232–244 (2008).
48. L. K. Carr, D. Steele, S. Steele, D. Wagner, R. Pruchnic, R. Jankowski, J. Erickson, J. Huard, and M. B. Chancellor. 1-year follow-up of autologous muscle-derived stem cell injection pilot study to treat stress urinary incontinence. *Int. Urogynecol. J*. **19**:881–883 (2008).
49. T. R. Payne, H. Oshima, M. Okada, N. Momoi, K. Tobita, B. B. Keller, H. Peng, and J. Huard. A relationship between vascular endothelial growth factor, angiogenesis, and cardiac repair after muscle stem cell transplantation into ischemic hearts. *J. Am. Coll. Cardiol*. **50**:1685–1687 (2007).